



## RESEARCH ARTICLE

# Dynamics of microRNA secreted via extracellular vesicles during the maturation of embryonic stem cell-derived retinal pigment epithelium

Dimitrios Pollalis<sup>1,2</sup> | Gopa Kumar Gopinadhan Nair<sup>1,2</sup> | Justin Leung<sup>1,3</sup> |  
 Clarisa Marie Bloemhof<sup>4,5</sup>  | Jeffrey K. Bailey<sup>6,7</sup> | Britney O. Pennington<sup>6,7</sup> |  
 Kaitlin R. Kelly<sup>6,7</sup> | Amir I. Khan<sup>6,7</sup> | Ashley K. Yeh<sup>7,8</sup> | Kartik S. Sundaram<sup>6,9</sup> |  
 Dennis O. Clegg<sup>6,7,9</sup> | Chen-Ching Peng<sup>1,10</sup> | Liya Xu<sup>1,10</sup>  | Constantin Georgescu<sup>11</sup> |  
 Jonathan D. Wren<sup>11</sup> | Sun Young Lee<sup>1,2,12</sup> 

<sup>1</sup>USC Roski Eye Institute, Keck School of Medicine, University of Southern California, Los Angeles, California, USA

<sup>2</sup>USC Ginsburg Institute for Biomedical Therapeutics, University of Southern California, Los Angeles, California, USA

<sup>3</sup>USC Dornsife College of Letters, Arts and Sciences, Los Angeles, California, USA

<sup>4</sup>University of Southern California, Los Angeles, California, USA

<sup>5</sup>School of Medicine, California University of Science and Medicine, Colton, California, USA

<sup>6</sup>Center for Stem Cell Biology and Engineering, Neuroscience Research Institute, University of California, Santa Barbara, California, USA

<sup>7</sup>Department of Molecular Cellular and Developmental Biology, University of California, Santa Barbara, California, USA

<sup>8</sup>College of Creative Studies, Biology, University of California, Santa Barbara, California, USA

<sup>9</sup>Biomolecular Science and Engineering, University of California, Santa Barbara, California, USA

<sup>10</sup>Children's Hospital Los Angeles Vision Center, Los Angeles, California, USA

<sup>11</sup>Genes & Human Diseases Research Program, Oklahoma Medical Research Foundation, Oklahoma City, Oklahoma, USA

<sup>12</sup>Department of Physiology and Neuroscience, Keck School of Medicine, University of Southern California, Los Angeles, California, USA

## Correspondence

Sun Young Lee, USC Roski Eye Institute, USC Ginsburg Institute for Biomedical Therapeutics and Department of Ophthalmology, Keck School of Medicine, University of Southern California, 1450 San Pablo, Los Angeles, CA 90033, USA.  
 Email: [SunYoung.Lee@med.usc.edu](mailto:SunYoung.Lee@med.usc.edu)

## Funding information

National Eye Institute, Grant/Award Numbers: R21EY035425, R01EY034193 (Lee Sun Young), P30EY029220; Alcon Research Institute; Young Investigator Award (Lee Sun Young); National Institutes of Health, Grant/Award Number: P30GM14376 (Wren Jonathan D.); Unrestricted Grant to the Department of Ophthalmology from Research to Prevent Blindness, New York, NY

## Abstract

Retinal pigment epithelial (RPE) cells are exclusive to the retina, critically multifunctional in maintaining the visual functions and health of photoreceptors and the retina. Despite their vital functions throughout lifetime, RPE cells lack regenerative capacity, rendering them vulnerable which can lead to degenerative retinal diseases. With advancements in stem cell technology enabling the differentiation of functional cells from pluripotent stem cells and leveraging the robust autocrine and paracrine functions of RPE cells, extracellular vesicles (EVs) secreted by RPE cells hold significant therapeutic potential in supplementing RPE cell activity. While previous research has primarily focused on the trophic factors secreted by RPE cells, there is a lack of studies investigating miRNA, which serves as a master regulator of gene expression. Profiling and defining the functional role of miRNA contained within RPE-secreted EVs is critical as it constitutes a necessary step in identifying the optimal phenotype of the EV-secreting cell and understanding the biological cargo of EVs to develop EV-based therapeutics. In this study, we present a comprehensive profile of miRNA in small

This is an open access article under the terms of the [Creative Commons Attribution-NonCommercial-NoDerivs License](https://creativecommons.org/licenses/by-nc-nd/4.0/), which permits use and distribution in any medium, provided the original work is properly cited, the use is non-commercial and no modifications or adaptations are made.

© 2024 The Author(s). *Journal of Extracellular Biology* published by Wiley Periodicals LLC on behalf of International Society for Extracellular Vesicles.

extracellular vesicles (sEVs) secreted during RPE maturation following differentiation from human embryonic stem cells (hESCs); *early-stage* hESC-RPE (20–21 days in culture), *mid-stage* hESC-RPE (30–31 days in culture) and *late-stage* hESC-RPE (60–61 days in culture). This exploration is essential for ongoing efforts to develop and optimize EV-based intraocular therapeutics utilizing RPE-secreted EVs, which may significantly impact the function of dysfunctional RPE cells in retinal diseases.

#### KEYWORDS

extracellular vesicle (EV), microRNA, retinal pigment epithelium (RPE), stem cell

## 1 | INTRODUCTION

Retinal pigment epithelium (RPE) is a monolayer of polarized cells uniquely located between the photoreceptors and the choroid vasculature within the chorioretina. These cells serve highly specialized functions in maintaining the health and visual functions of photoreceptors and the retina, including conservation of the visual cycle, protection against oxidative stresses, secretion of cytokines and growth factors, maintain blood retinal barrier (BRB) and transportation of nutrients (Strauss, 2005). Given their postmitotic status and the demanding roles they play throughout the lifetime, the RPE is particularly susceptible to pathology in major blinding retinal degenerative conditions such as age-related macular degeneration (AMD) (Campello et al., 2021; Handa et al., 2019).

Benefiting from the advancements in stem cell technology enabling the differentiation of functional cells from pluripotent stem cells (PSC) or induced PSC (iPSC) and leveraging the robust autocrine and paracrine functions of RPE cells, extracellular vesicles (EVs) secreted from RPE cells hold significant therapeutic potential in supplementing RPE cell activity. Studies have shown that stem cell-derived polarized RPE cells exhibit both phenotypic and functional similarities to RPE cells obtained from human retina tissues (Croze et al., 2014; Leach et al., 2016; Petrus-Reurer et al., 2022). These fully differentiated and polarized RPE cells have demonstrated proven intraocular safety profiles and functional integration in ongoing human clinical trials involving cell transplantation (Kashani et al., 2018, 2021; Mandai et al., 2017; Mehat et al., 2018; Schwartz et al., 2015). Our group recently reported that concentrated cell culture conditioned media (CCM) of hESC-derived fully differentiated and polarized RPE promoted retinal progenitor cell survival, reduced oxidative stress in APRE-19 cells, and preserved PR and their function in the Royal College of Surgeons (RCS) rat model (Ahluwalia et al., 2023). Accumulating evidence suggests that cell-secreted small extracellular vesicles (sEVs) play a crucial role in facilitating cell-to-cell communication. sEV carries essential biological cargos such as proteins, lipids, and microRNAs (miRNA), which are encapsulated and protected by a lipid bilayer membrane of sEV from nucleases, proteases, changes in pH or osmolarity (Ludwig & Giebel, 2012; Ratajczak et al., 2006; van der Pol et al., 2012). Taking advantage of advancements in high-throughput technologies, such as proteomics, microarray, RNA-Seq and ChIP-Seq, systematic analysis of EV cargo has been enabled (Kim et al., 2017; Vaka et al., 2023). However, studies on miRNA secreted from RPE are lacking, especially during their maturation followed by differentiation from PSCs while RPE-secreted proteomics has been relatively well defined (Flores-Bellver et al., 2021; Georgi & Reh, 2010; La Torre et al., 2013; Meyer et al., 2019; Wright et al., 2020; Yuan et al., 2015).

miRNAs are small (~22 nucleotides) noncoding, highly conserved, single-stranded RNAs known to play an important role in various biological processes by directly or indirectly regulating the expression of target mRNAs (Carthew & Sontheimer, 2009; Kim, 2005). Approximately 2200 miRNA genes have been reported to exist in the mammalian genome and the expression of miRNAs is tightly regulated, showing dependence on developmental stage and tissue specificity (Ardekani & Naeni, 2010; Lagos-Quintana et al., 2002). Furthermore, their association with retinal health and diseases has been demonstrated (Georgi & Reh, 2010; La Torre et al., 2013; Wright et al., 2020; Yuan et al., 2015). Thus, the miRNA cargo of EVs represents a potentially critical component of the functional role of RPE-secreted EVs in therapeutics. Profiling and understanding the functional role of miRNA contained within RPE-secreted EVs are critical steps in identifying the optimal phenotype of the EV-secreting cell and understanding the biological cargo of EVs to develop EV-based therapeutics.

RPE maturity has been reported to affect cellular pigmentation and the production of several functional proteins such as pigment epithelium-derived factor (PEDF), bestrophin-1 (BEST1) and cellular retinaldehyde-binding protein (CRALBP). Previous studies have demonstrated that in vitro maturation of hESC-derived RPE cells continues for 8 weeks with increasing expression of key functional genes (Bennis et al., 2017; Dunn et al., 1996; German et al., 2008). Interestingly, transplantation of hESC-derived RPE obtained after 4 weeks of culture showed a better vision-rescuing effect in animal models compared to those cultured for 2 or 8 weeks (Al-Ani et al., 2020; Davis et al., 2017). This suggests that the optimal phenotype of the cells needs to be assessed based on the therapeutic strategy employed, such as cell implantation or cell-secreted EVs.

In this study, we present a comprehensive miRNA profiling in sEVs secreted during the maturation of RPE after differentiation from hESC; *early-stage* hESC-RPE (20–21 days in culture), *mid-stage* hESC-RPE (30–31 days in culture) and *late stage* hESC-RPE (60–61 days in culture). Additionally, we conducted associated pathway analyses to gain insights into the functional roles of these profiled miRNAs. Our findings contribute to bridging the existing knowledge gap and lay the foundation for further exploration of RPE-secreted EV therapeutics.

## 2 | RESULT

### 2.1 | hESC-RPE characterization

The fully differentiated hESC-RPE cells, regardless of their maturation status, exhibited RPE cell characteristics, including distinctive ZO-1-positive cobblestone and hexagonal morphology. Meanwhile, the pigmentation grading increased with maturation across three groups, *early-stage* (20–21 days in culture), *mid-stage* (30–31 days in culture) and *late-stage* (60–61 days in culture) (Figure 1a). Additionally, immunofluorescence analysis of hESC-RPE cells, stained with anti-BEST1 and anti-RPE65 antibodies, revealed maturation-dependent variations. These differences were further confirmed through qPCR-based evaluation of gene expression, with BEST1 expression levels being 31.8-fold, 46.2-fold and 28.9-fold increase over the reference genes for *early-stage*, *mid-stage* and *late-stage* hESC-RPE, respectively, and RPE65 expression levels being 0.12-fold, 0.3-fold and 0.28-fold increase over the reference genes for *early-stage*, *mid-stage* and *late-stage* hESC-RPE, respectively (Figure 1b,c).

hESC-RPE cells presented fully differentiated distinctive RPE characteristics, with increased pigmentation observed over RPE cell maturation, along with a decrease in their proliferation in cell culture (data not shown), with days of gap between the groups to minimize potential molecular overlapping.

### 2.2 | hESC-RPE-sEVs biophysical characteristics

The quantification and characterization of the hESC-RPE-sEVs were performed using nanoparticle tracking analysis (NTA) with NanoSight. Notably, the particle numbers of sEV released by *early-stage* hESC-RPE exceeded those of the other groups, with counts for *early-*, *mid-* and *late-stage* hESC-RPE-sEVs measured at  $4.42 \times 10^{11}$  ( $\pm 1.14 \times 10^{11}$ ),  $1.56 \times 10^{11}$  ( $\pm 2.25 \times 10^{10}$ ) and  $1.94 \times 10^{11}$  ( $\pm 3.50 \times 10^{10}$ ) particles/mL, respectively (Figure 2d). The average size of sEV was comparable with 113, 108 and 117 nm in *early-*, *mid-* and *late-stage* hESC-RPE-sEVs, respectively, and their morphology observed in TEM images from the three age groups was comparable (Figure 2a).

### 2.3 | Exosomal tetraspanins and surface epitopes of hESC-RPE-sEV

The tetraspanin distribution in sEV, as analyzed by ExoView, remained consistently similar across different maturation stages of the hESC-RPE cells (Figure 2b). In-depth surface protein epitopes capturing 37 distinct surface markers identified predominant surface proteins across different age groups, including ROR1, CD9, CD63, CD81, CD133/1 and CD29 (Figure 2c).

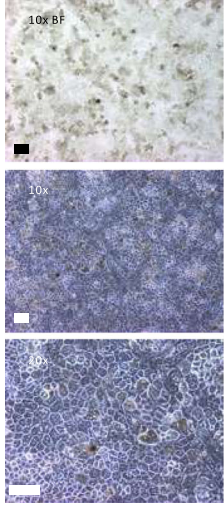

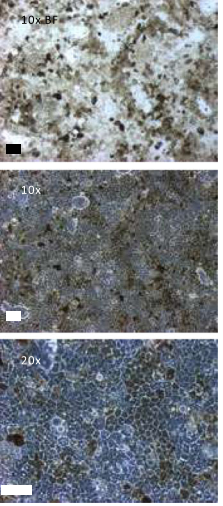
### 2.4 | Purity, protein and RNA concentration in hESC-RPE-sEVs

The protein concentration averaged 0.17, 0.11 and 0.20 mg/mL in *early-*, *mid-* and *late-stage* hESC-RPE-sEVs, respectively (Figure 2e). Further analysis of the sEV purity index (particle-to-protein ratio) was found to be high values across all groups, with highest in the *early-stage*:  $2.70 \times 10^9$ ,  $1.55 \times 10^9$  and  $9.48 \times 10^8$  P/mg in *early-*, *mid-* and *late-stage* hESC-RPE-sEVs, respectively (Figure 2f). The total RNA concentration was  $2.79 \times 10^5$ ,  $1.14 \times 10^5$  and  $1.24 \times 10^5$  pg/mL in the *early-*, *mid-* and *late-stage* hESC-RPE-sEVs, respectively (Figure 2g). RNA-to-Particle ratio was comparable among the groups ( $6.59 \times 10^{-7}$ ,  $7.68 \times 10^{-7}$  and  $6.28 \times 10^{-7}$  pg/particle in *early-*, *mid-* and *late-stage* hESC-RPE-sEVs, respectively) (Figure 2h).

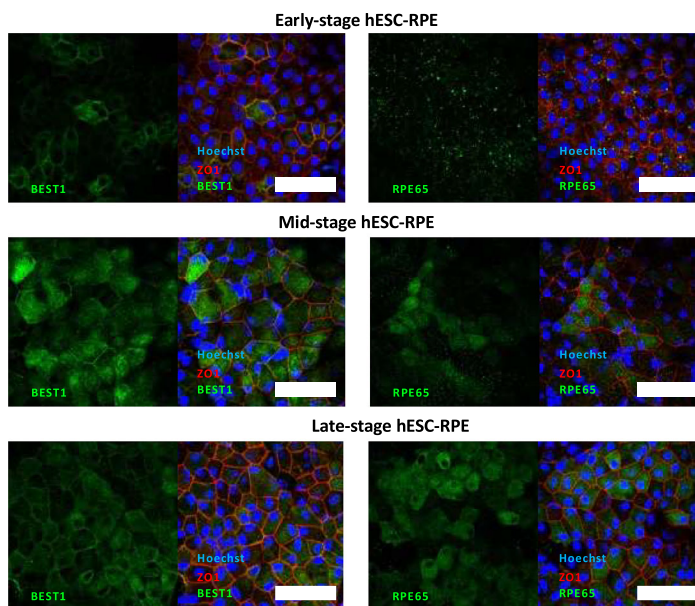
### 2.5 | microRNA profiles in sEV during hESC-RPE maturation

The miRNA profiles of hESC-RPE-sEVs exhibited notable distinctions across the three groups of hESC-RPE cells (Figure 3a, Table S1). In the overall miRNA expression pool, comprising 210 miRNAs (Ct  $\leq$  30), varying counts were observed in sEV derived from *early-*, *mid-* and *late-stage* hESC-RPE cells, with totals of 80, 199 and 166 miRNAs, respectively (Figure 3a). Two miRNAs were shared only by *early-stage* and *mid-stage* hESC-RPE-sEVs and 1 miRNA was shared only by *early-stage* and

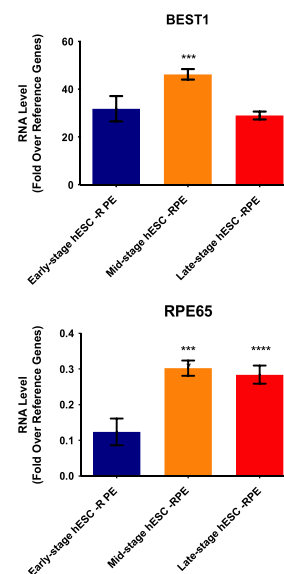
(a)

	Early-stage hESC-RPE	Mid-stage hESC-RPE	Late-stage hESC-RPE
Days in culture	20-21	30-31	60-61
RPE pigmentation grade	1	2	3-4
RPE morphology	hexagonal	hexagonal	hexagonal
RPE confluency	95-100%	95-100%	95-100%
			

(b)

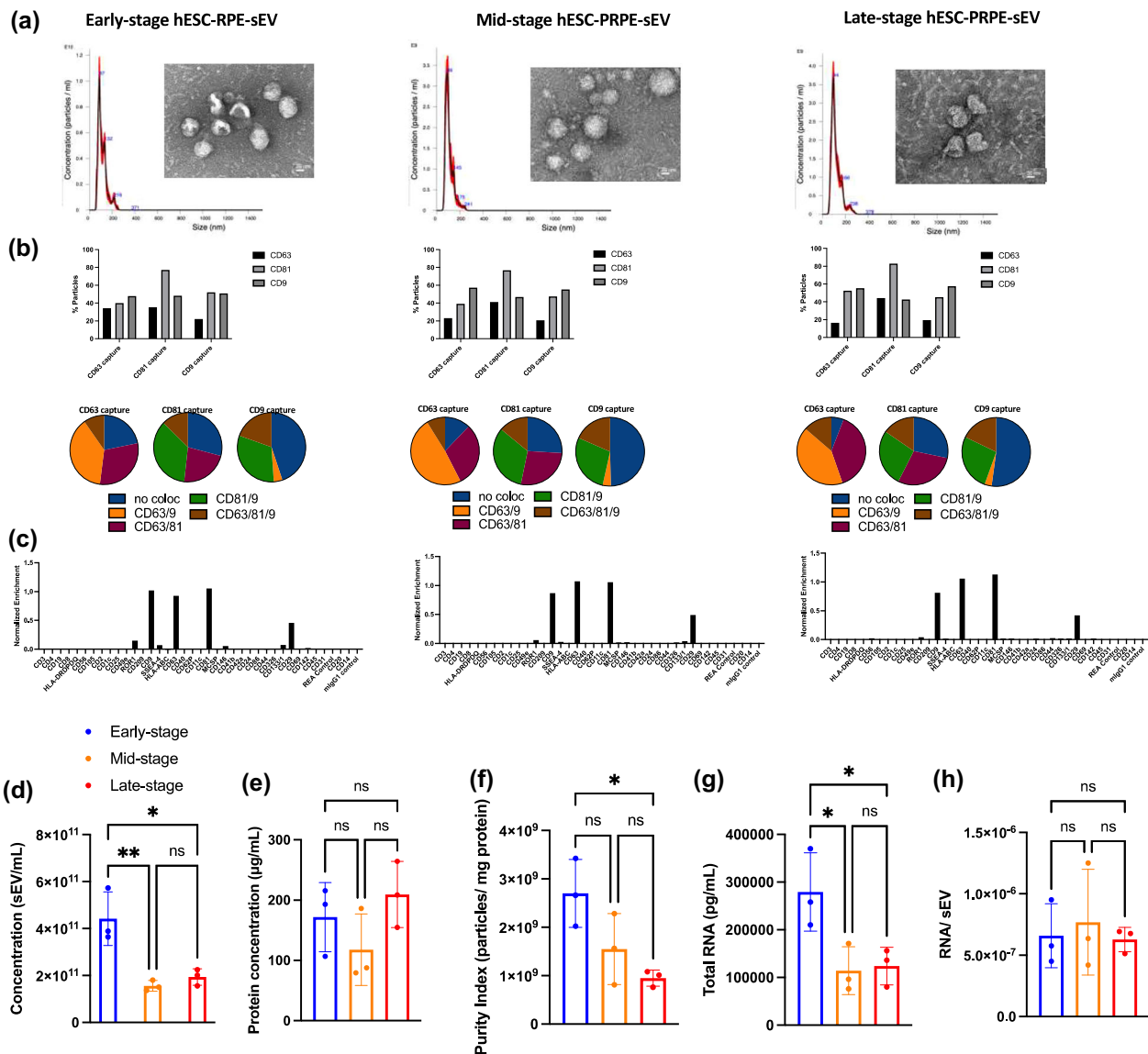


(c)



**FIGURE 1** Characterization of human embryonic stem cell-derived retinal pigment epithelial cells during cell maturation. (a) Summary table of the phenotypical characteristics of *early*-, *mid*-, and *late*-stage in cultured hESC-RPE cells and representative brightfield and phase-contrast images (scale bar, 100  $\mu$ m). (b) Representative images of hESC-RPE cells stained with anti-BEST1, RPE65, and ZO-1 antibodies (scale bar, 50  $\mu$ m). (c) BEST1 expression was increased in *early*-stage hESC-RPE compared to the other two age groups, while RPE65 expression was found to be increased with cell culture time. \*\*\* $p < 0.001$ , \*\*\*\* $p < 0.0001$ .

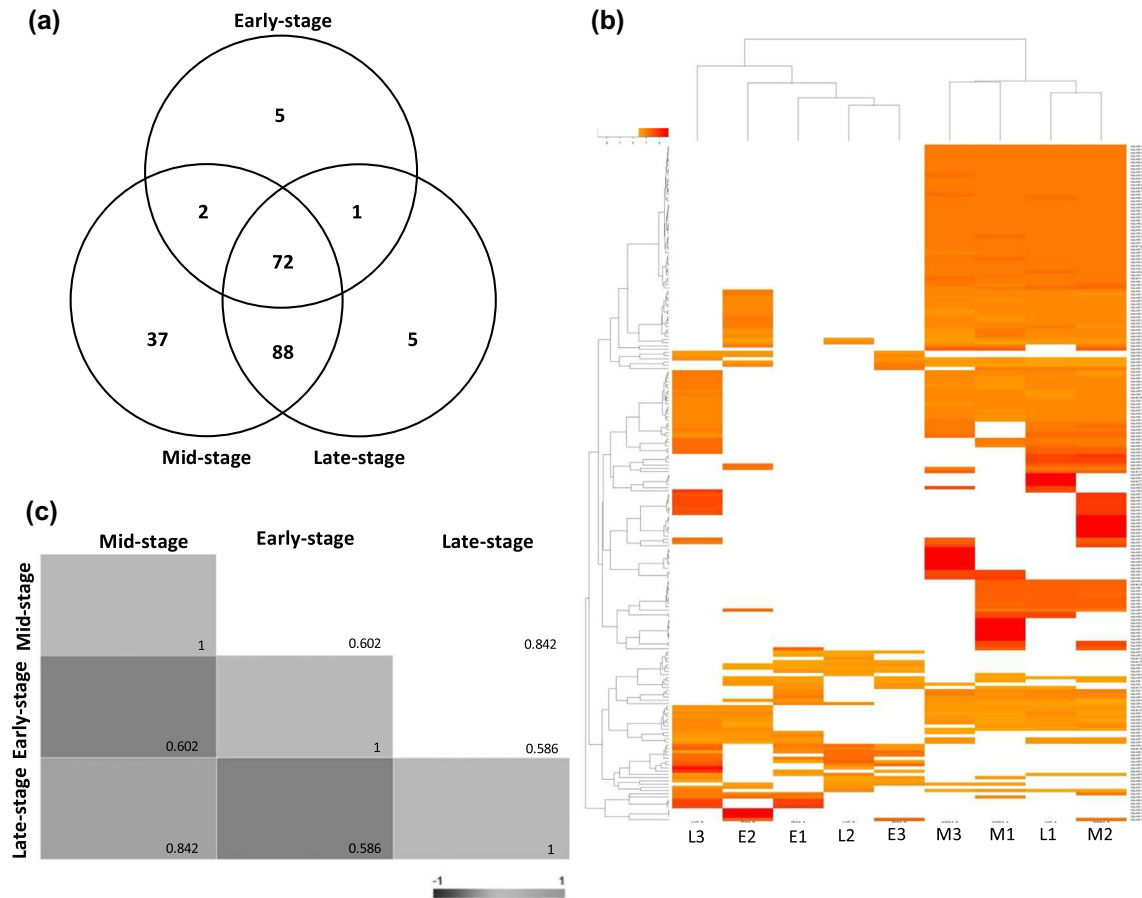
*late*-stage hESC-RPE-sEVs, while 88 miRNAs were shared exclusively between *mid*-stage and *late*-stage hESC-RPE-sEVs. *Early*-, *mid*- and *late*-stage hESC-RPE-sEVs exhibited unique expression patterns for 5, 37 and 5 miRNAs, respectively. A non-supervised hierarchical clustering of all expressed miRNAs (Ct  $\leq$  30), revealed a distinct separation of the *mid*-stage hESC-RPE-sEVs group from the other two groups while the correlation plot showed that the *late*-stage hESC-RPE-sEVs group was more closely related to the *mid*-stage group than to the *early*-stage hESC-RPE-sEVs group (Figure 3b,c).



**FIGURE 2** Biophysical characterization of sEV secreted from human embryonic stem cell-derived retinal pigment epithelial cells during maturation. (a) Representative size versus concentration distribution graphs of sEV derived from the three groups of hESC-RPE cells ( $N = 3$ ) as analyzed by NanoSight and representative transmission electron microscopy (TEM) images of sEV providing a visual comparison (scale bar, 20 nm). (b) Distribution and colocalization analysis of tetraspanins (CD81, CD9, and CD63) within sEV derived from the three age groups of hESC-RPE cells. (c) Results from the MACSPlex assay conducted on early-, mid-, and late-stage hESC-RPE-sEV. Comparisons of: (d) sEV concentration, (e) protein concentration, (f) purity index (particle-to-protein ratio), and (g) total RNA and (h) RNA-to-sEV particle ratio among the three groups of hESC-RPE-sEV. Data are presented as mean  $\pm$  standard deviation (SD). \* $p < 0.05$ , \*\* $p < 0.01$ .

## 2.6 | Pathway analysis

To investigate the functional implications of highly expressed miRNAs with cut off Ct value of 25, we identified a total 25 miRNAs with Ct  $\leq 25$ , which were differentially expressed across the three groups (Figure 4a). Overall, the *mid-stage* hESC-RPE-sEVs group exhibits a rich expression of these miRNAs, with 22 out of 25 being highly expressed, compared to 6 out of 25 in the *early-stage* and 5 out of 25 in the *late-stage* hESC-RPE-sEVs groups. We also identified the target genes of these 25 miRNAs using Ingenuity Pathway Analysis (IPA) (Figure 4b). Furthermore, using IPA, we predicted target pathways for the 25 miRNAs with Ct  $\leq 25$ , identifying 463 statistically significant distinct pathways (data not shown). Our detailed examination, focusing on extracellular vesicle- and retina-related pathways, revealed major associations with regulatory networks governing extracellular vesicle trafficking, tissue and cellular polarity, growth factor regulation, inflammation, and oxidative stress and senescence. Although we observed that all these pathways were involved in miRNAs across the three groups of hESC-RPE, the miRNAs contained in



**FIGURE 3** MicroRNA profiles of sEV secreted from human embryonic stem cell-derived retinal pigment epithelial cells during maturation. (a) Venn diagram of the total number of miRNAs ( $Ct \leq 30$ ) identified in the sEV of the three hESC-RPE maturation groups ( $N = 3$ ). (b) Heatmap of the expressed miRNAs ( $Ct \leq 30$ ) in hESC-RPE-sEV throughout RPE maturation in culture. (c) Correlation plot of the three hESC-RPE-sEV groups.

mid-stage hESC-RPE were heavily involved in these pathways with statistical significance. The downstream pathways under each focused pathway were selected based on the statistically significant involvement of miRNAs from the three groups (Figure 5 a–i, b–i, c–i, d–i and e–i).

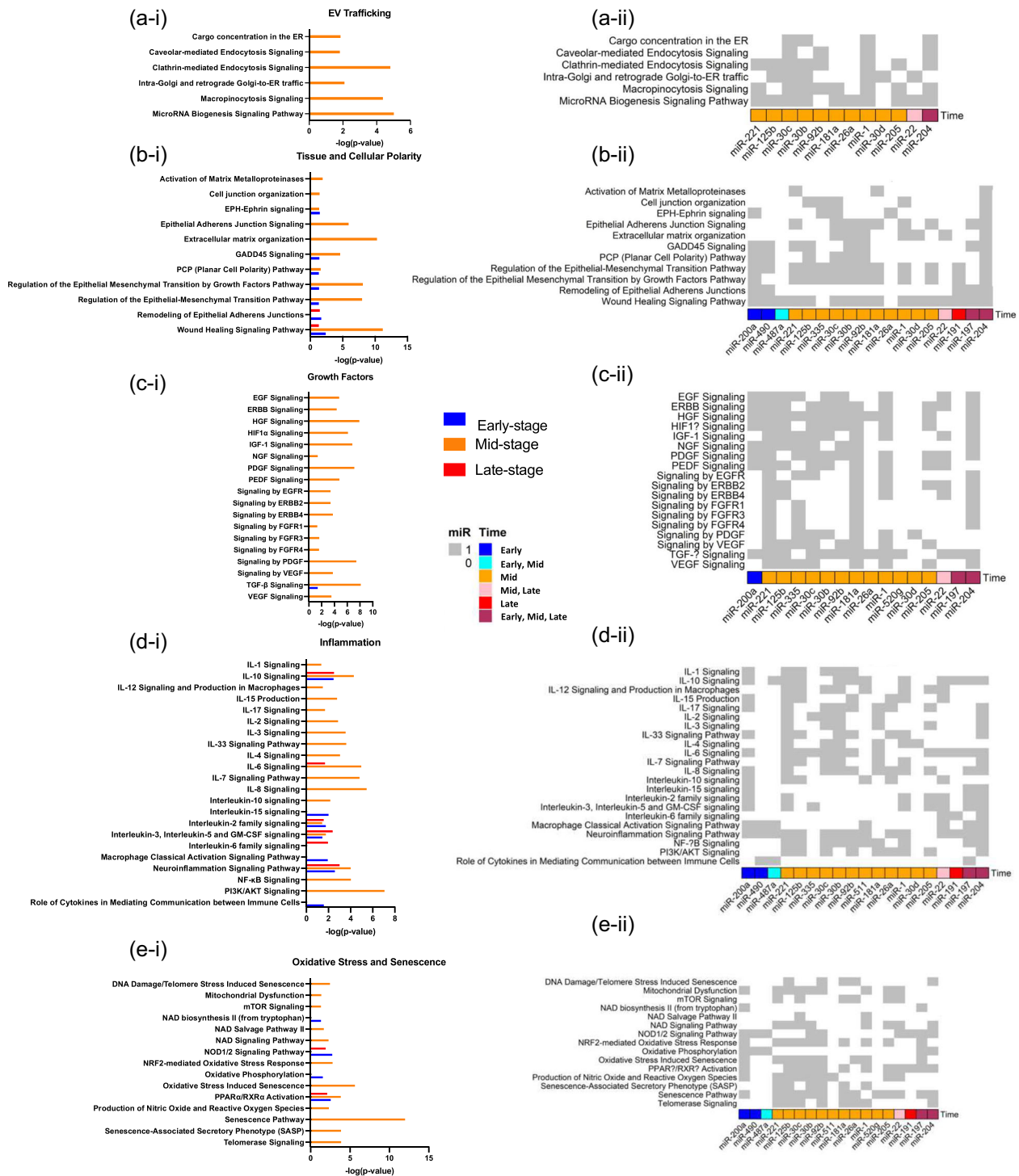
To overcome the current limitation of IPA in associating individual miRNAs with focused pathway analyses, we employed In-Silico Construction of an Entity-based Network from Text (IRIDESCENT) (Wren et al., 2004; Wren & Garner, 2004). Through IRIDESCENT analysis, we identified the relationship between single miRNAs among the 25 miRNAs with  $Ct \leq 25$  and each focused pathway (Figure 5 a–ii, b–ii, c–ii, d–ii and e–ii).

### 3 | DISCUSSION

Several previous studies have reported variability in cellular miRNA expression during the differentiation of RPE from stem cells, as well as the involvement of different target miRNAs from the RPE in mediating retinal diseases (Ahn et al., 2021; Guo et al., 2023; Morris et al., 2020; Wooff et al., 2020). However, to the best of our knowledge, our study is the first to conduct a comprehensive analysis of the miRNA profile contained in sEVs secreted from hESC-RPE during their maturation. As stem cell-derived RPE cell therapy advances toward clinical application, research has revealed the in vitro cellular maturation of stem cell-derived RPE, which can extend up to 8 weeks in culture. Interestingly, their therapeutic efficacy in vivo appears to be better in cells cultured for 4 weeks (Schwartz et al., 2015; Mehat et al., 2018; Mandai et al., 2017; Kashani et al., 2018, 2021; Al-Ani et al., 2020; Davis et al., 2017). However, there is a lack of studies focusing on determining the optimal phenotype of sEV secreted from RPE and understanding the biological cargo of sEVs to develop RPE secreted EV-based therapeutics.

Our study results reveal an interesting finding that the number of recovered sEVs from *early-stage* hESC-RPE, while maintaining similar cell culture numbers and the same volume input of CCM, was significantly higher compared to *mid-stage* and *late-stage* hESC-RPE (Figure 2d). This observation suggests that sEV secretion is regulated during cell maturation. While the





**FIGURE 5** Associated pathway analyses of the highly expressed microRNAs in sEV secreted from human embryonic stem cell-derived retinal pigment epithelial cells during maturation. The expressed miRNAs with Ct  $\leq$  25 in the three hESC-RPE maturation groups ( $N = 3$ ) were analyzed via Ingenuity Pathway Analysis (IPA) (i) and In-Silico Construction of an Entity-based Network from Text (IREDESCENT) (ii), focusing on pathways related to: (a) EV trafficking, (b) tissue/cellular polarity, (c) growth factors, (d) inflammation and (e) oxidative stress and senescence.  $-\text{Log}(p\text{-value}) > 1.3$  is considered statistically significant. culture days of 30–31 than the early-stage culture days of 20–21. It is intriguing that *early-stage* hESC-RPE secreted more sEVs; however, their cargo, including protein or RNA amounts, was comparable, and their microRNA cargo was less variable which may will require future study for its biological implication. Furthermore, it remains unknown whether all sEVs in a population contain the same amount or the same kind of microRNAs, or if some vesicles are selectively loaded with specific microRNAs, given the heterogeneity of cell-secreted sEVs and the limitations of current technology. Despite these limitations stemming from current technological constraints, our study results provide valuable information on the greater variety of miRNAs secreted from *mid-stage* hESC-RPE-sEVs.



In the pathway analysis to determine the molecular pathways involved in these differentially expressed miRNAs at each stage of hESC-RPE-sEVs, we analyzed the functional implications of highly expressed miRNAs with a cut-off Ct value of 25. We identified a total of 25 miRNAs with Ct  $\leq$  25, which were differentially expressed across the three groups. Similar to the total miRNA pools, the *mid-stage* hESC-RPE-sEVs group exhibited a rich expression of these miRNAs, with 22 out of 25 being highly expressed, compared to 6 out of 25 in the *early-stage* and 6 out of 25 in the *late-stage* hESC-RPE-sEVs groups. We also identified the target genes of these 25 miRNAs using Ingenuity Pathway Analysis (IPA) (Figure 4). To further investigate the functional roles of the highly expressed 25 miRNAs contained in hESC-RPE-sEVs, we identified 463 statistically significant distinct pathways (data not shown) using IPA. Out of the total 463 different pathways identified from the highly expressed 25 miRNAs, our focused analysis on pathways related to “EVs” or “retina” revealed several significant pathways. Specifically, EV trafficking, tissue and cellular polarity, growth factor regulation, inflammation, and oxidative stress and senescence emerged as major pathways associated with EVs and the retina. The downstream pathways under each focused pathway were also selected based on the statistically significant involvement of miRNAs from the three groups. Although many of these pathways involved miRNAs across the three groups of hESC-RPE, the miRNAs contained in *mid-stage* hESC-RPE were more broadly involved in these pathways with statistical significance than in sEVs from *early-* or *late-stage* (Figure 5a). To overcome the current limitation of IPA in associating individual miRNAs with focused pathway analyses, we employed In-Silico Construction of an Entity-based Network from Text (IRIDESCENT) (Wren et al., 2004; Wren & Garner, 2004). Through IRIDESCENT analysis, we identified the relationship between individual miRNAs among the 25 miRNAs with Ct  $\leq$  25 and each focused pathway, which also confirms that miRNAs contained in sEVs from *mid-stage* hESC-RPE were more broadly involved in these five major pathways (Figure 5b).

These results indicate that miRNAs contained in sEVs secreted by hESC-RPE cells are involved in known RPE functions. Additionally, hESC-RPE cells in their *mid-stage* (30–31 days in culture) release sEVs with more variable miRNA profiles associated with enriched RPE functions. With the excitement surrounding the abundance of miRNAs associated with essential RPE functions contained in RPE-sEVs from our study results, the key question regarding the therapeutic relevance of EV miRNAs needs to be further verified. The current study cannot verify whether these pathways are protective or detrimental to retinal health (e.g., in inflammation or oxidative stress) (Bian et al., 2020; Ke et al., 2021; Mathew et al., 2019). Further studies are also needed to investigate the capacity to initiate phenotypic effects in recipient cells through cytoplasmic delivery. Joshi et al. and Bonsergent et al. reported that approximately 10%–30% of internalized EVs released cargo to the cytoplasm, as indicated by their reporter system (Bonsergent et al., 2021; Joshi et al., 2020). de Jong et al. (2020) observed that the functional transfer of RNA varied based on the combination of donor and receptor cells, while it was also shown that EV-delivered miRNAs could participate in mRNA suppression (Abels et al., 2019). Therefore, there is great therapeutic potential for miRNAs contained in EVs. Our study results and ongoing human clinical trials using hESC-RPE cells with similar cell phenotypes (cultured for around 4 weeks) and the protective therapeutic efficacy observed in pre-clinical studies support the therapeutic relevance of these miRNAs and the rationale for optimizing cell culture conditions to capitalize on the rich miRNA cargo contained in sEVs when considering sEV therapy (Schwartz et al., 2015; Mehat et al., 2018; Mandai et al., 2017; Kashani et al., 2018, 2021; Al-Ani et al., 2020; Davis et al., 2017).

Previous profiling of the differentially expressed miRNAs in RPE cells during their differentiation, either from hESC or iPSC, has studied the various roles of miRNAs in RPE, such as differentiation, proliferation, migration, homeostasis, the visual cycle, phagocytosis and cell clearance (Intartaglia et al. 2021; Wang et al., 2014; Yuan et al., 2015). It is difficult to directly compare miRNA profiling between previous studies on RPE cells and our results in hESC-RPE-sEV due to different profiling methodologies and data analyses. However, some of the 25 highly expressed miRNAs identified in hESC-RPE-sEVs, such as miR-204-5p and miR-211-5p, have also been identified as major cellular miRNAs of RPE cells. Members of the miR-204/211 family are arguably the most extensively studied miRNAs in the RPE. Previous studies have shown that miR-204/211 are involved in various critical functions in RPE cells, including regulating RPE cell differentiation, proliferation, and homeostasis. For instance, miR-204 knockout (KO) and miR-211 knockout (KO) studies have demonstrated their essential roles in regulating RPE cell differentiation, proliferation and homeostasis (Barbato et al., 2017; Wang et al., 2010; Zhang et al., 2019)

Additionally, our study highlights the differentially expressed miRNAs profiled within the sEVs from hESC-RPE compared to the major miRNA content within hESC-RPE, aligning with the current understanding that cellular miRNAs and EV-mediated miRNAs are differently regulated (Yuan et al., 2015). While the precise functional role of miRNAs contained in hESC-RPE-sEVs requires further exploration in specific signalling contexts, our pathway analyses support at least three potential roles for these miRNAs. First, they may be involved in EV machinery as EV resident miRNAs, contributing to processes such as EV trafficking, which involves three main mechanisms for EV-RNA uptake: cell surface membrane fusion, cell contact-dependent mechanisms and endocytic pathways (including clathrin-mediated, caveolin-dependent, receptor-mediated endocytosis, micropinocytosis, and phagocytosis). Second, these miRNAs may contribute to RPE cell health by impacting tissue and cellular polarity, suggesting that secreted miRNAs may mediate the microenvironment and/or health of RPE through autocrine and/or paracrine effects. Third, miRNAs might play a role in multiple pathways associated with essential RPE functions, such as growth factor regulation, inflammation and oxidative stress. Consequently, miRNAs in hESC-RPE-sEVs could participate in both EV machinery-related processes and functional roles of the RPE through sEV-mediated autocrine and paracrine actions of RPE cells.

This study has limitations. The assessment was conducted under uniform cell culture conditions; however, it is possible that in vivo RPE-secreted sEVs have different miRNA profiles reflecting the microenvironment. As defining the optimal in vitro cell

culture conditions to produce miRNA-rich sEVs for RPE-sEVs therapeutics is a necessary step, it would be beneficial to investigate miRNA profiling of sEVs from RPE exposed to various conditions. Another important future study aspect is assessing and predicting the multidimensional synergistic benefits of EV therapy when multiple molecules simultaneously affect the microenvironment. Multimolecular (e.g., protein and miRNA)-based sEVs therapeutics may offer synergistic benefits beyond the single molecule-driven therapy to the biological system. Next-generation integrative pathway enrichment analysis of multivariate omics data will likely be necessary to address this gap. Furthermore, our study results are specific to hESC-derived RPE, and a separate investigation will be required for iPSC-derived RPE, another prevalent source.

In summary, the miRNAs found in hESC-RPE-sEVs reveal their potential diverse roles, from aiding in vesicle movement to supporting cell health and participating in essential RPE cellular functions. The differences between vesicle miRNA content from our study and cellular miRNA from previous studies highlight the unique way these vesicles sort their cargo. While our study provides important insights into identifying the optimal phenotype of the EV-secreting cell, more research is needed to fully understand how these miRNAs work and their potential effects. Exploring these complexities could lead to innovative treatments for various diseases, making vesicle-delivered miRNAs a promising area for future therapies for retinal diseases.

## 4 | MATERIAL AND METHODS

### 4.1 | hESC-RPE cell differentiation, and culture

Human embryonic stem cells (WA09, WiCell Research Institute) were spontaneously differentiated into RPE cells as previously described (Leach et al., 2016). Briefly, colonies of hESCs were manually passaged, seeded onto tissue culture plates coated with Matrigel hESC-Qualified Matrix (Corning #354277), and received biweekly medium exchanges of XVIVO-10 medium (Lonza # (BE) BP04-743Q) for approximately 3 months. Pigmented regions were then manually isolated, expanded for two passages, and cryopreserved at 2–5 days post-seed as a cellular suspension using CryoStor10 cryopreservation medium (BioLife Solutions #210102). Thawed cells were expanded using 10 mM Y-27632 (Tocris #1254) until the eighth passage as previously described (Croze et al., 2014). Cultures were tested every other month using MycoAlert Mycoplasma Detection Kit (Lonza LT07-318) and determined to be negative for mycoplasma throughout the study.

### 4.2 | Pigmentation assessment

Upon reaching confluence, for each age group, representative fields of view were acquired by bright field and phase contrast microscopy using an Olympus CK40 inverted microscope and Infinity Capture software. Upon reaching confluence, pigmentation in hESC-RPE cells was categorized as follows: grade 0—pigmentation in 0%–10% of the total area, grade 1—pigmentation in 11%–25% of the total area, grade 2—pigmentation in 26%–50% of the total area, grade 3—pigmentation in 50%–80% of the total area and grade 4—pigmentation in >80% of the total area (Pollalis et al., 2024).

### 4.3 | Immunocytochemistry and confocal fluorescence microscopy

hESC-RPE were cultured on sterile, matrigel-coated, #1.5 coverslips (GG121.5PRE, Neuvitro) before fixation with 4% methanol-free formaldehyde in PBS for 20 min. Cells were subsequently permeabilized with 0.1% Triton X-100 for 10 min, blocked with 5% goat serum (Jackson ImmunoResearch) and 1% BSA (Thermo Fisher Scientific) in PBS for 30 min, and incubated in the following primary antibodies overnight at 4°C: rabbit-anti-ZO-1 (40-2200, Thermo Fisher Scientific, 1:200) and mouse-anti-RPE65 (MAB5428, Millipore-Sigma, 1:200). Coverslips were washed three times with PBS followed by secondary antibody incubation in blocking buffer for 1 h at room temperature. Secondary antibodies were: AlexaFluor 594 AffiniPure goat anti-rabbit IgG (111585144, Jackson ImmunoResearch, 1:200) and AlexaFluor 488 AffiniPure goat anti-mouse IgG (115545062, Jackson ImmunoResearch, 1:200). Nuclei were stained for 10 min with Hoechst 33342 in PBS (2 µg/mL), washed three times with PBS, mounted in ProLong Gold antifade, and imaged on an Olympus FV1000 Spectral Confocal with a PLAPON-SC 60X oil objective (NA: 1.40), and excitation laser lines at 405, 488, 559 and 635 nm. ImageJ-FIJI (NIH, USA) was used to generate single confocal planes extracted from z-stacks.

### 4.4 | RT-qPCR of hESC-RPE cells

Lysates for RNA purification were prepared by aspirating growth medium and triturating hESC-RPE cultures in RLT Buffer (Qiagen) followed by storage at –80°C. RNA was purified using RNeasy columns (Qiagen) and included an on-column genomic DNA

digestion step using RNase-free DNase (Qiagen). Reverse transcription and PCR were performed on 35ng of total RNA per well using AgPath-ID One-Step RT-PCR Reagents (4387424, Thermo Fisher Scientific) with the following TaqMan primer-probe sets (all Thermo Fisher Scientific): EIF2B2 (Hs00204540\_m1), SERF2 (Hs00428481\_m1), UBE2R2 (Hs00215107\_m1), BEST1 (Hs00188249\_m1) and RPE65 (Hs01071462\_m1). All Ct data were first linearized ( $2^{-Ct}$ ), and values for RPE65 and BEST1 were normalized to the geometric mean of the three reference genes (EIF2B2, SERF2 and UBE2R2).

#### 4.5 | Preparation of conditioned cell culture medium

To generate conditioned cell culture medium (CCM) from hESC-RPE, RPE cells were enzymatically passaged using TrypLE Select (Gibco #12563011) per manufacturer's instructions and seeded onto tissue culture plates coated with Matrigel hESC-Qualified Matrix (Corning #354277) at a density of 70,000 cells/cm<sup>2</sup>. The viability of the cells at the time of plating was determined by trypan blue exclusion, and cultures exceeding 95% viability were used for the study. At one day post-seed, cells were rinsed with DPBS (Gibco #14040141) and fed with 4mL EV-free XVIVO-10 medium (Lonza #(BE)BP04-743Q) per well within a 6-well tissue culture plate. The medium was exchanged twice per week and was supplemented with 10  $\mu$ M Y-27632 (Tocris #1254) for 10–15 days until the RPE cells attained cuboidal morphology. Starting at 20 until 61 days post-seed, CCM was collected from four wells of a 6-well plate using a serological pipet, combined, and immediately frozen in a 50 mL Falcon centrifuge tube at  $-80^{\circ}\text{C}$  until future use. Four replicate plates were used at each collection time point. Three replicate ( $N = 3$ ) samples were collected for each time point. The incubation period in which cells conditioned the medium ranged from 3 to 4 days at  $37^{\circ}\text{C}$ , 5%  $\text{CO}_2$ . The three distinct groups were selected based on RPE pigmentation, RPE65, BEST1 and PEDF expression: *early*- hESC-RPE (20–21 days in culture), *mid*- hESC-RPE (30–31 days in culture), and *late*-stage in culture hESC-RPE (60–61 days in culture).

#### 4.6 | Small extracellular vesicle recovery

For sEV recovery, ExoDisc<sup>®</sup> (LabSpinner, Ulsan, South Korea), a microfluidic tangential flow filtration method-based equipment was used following the manufacturer's instructions (Leung et al., 2024; Woo et al., 2017; Dong et al., 2020). In brief, an input volume of 3 mL of each test article (*early*-hESC-RPE, *mid*-hESC-RPE and *late*-stage culture hESC-RPE) was processed on an ExoDisc<sup>®</sup> using the bench-top operating machine (OPR-1000, LabSpinner<sup>™</sup>, South Korea). Purified sEV were retrieved from the collection chamber using 100  $\mu$ L of PBS and immediately stored at  $-80^{\circ}\text{C}$  until further use within 1–2 weeks.

#### 4.7 | Biophysical particle analysis

The concentration and size distribution of recovered sEV were measured by NanoSight (Malvern Panalytical, UK), following the manufacturer's protocol. In brief, for NanoSight (NS) analysis, the samples were diluted to obtain the optimal detection concentration of  $10^8$  particles/mL; an automated syringe pump was used to achieve a constant flow speed of 25, and five videos were captured using camera level 14. The data were analyzed using NTA software 4.3 with detection threshold 7 and adjusted by the dilution factor.

#### 4.8 | Transmission electron microscopy

sEV were visualized by negative-stained transmission electron microscopy (TEM) using a JEOL JEM-2100 microscope mounted on a Gatan OneView IS camera. Thin formvar/carbon-coated EM grids (Ted Pella, Inc.) were loaded with 6  $\mu$ L diluted sEV solution, incubated for 4 min, excess solution wicked and stained with 10  $\mu$ L 4% uranyl acetate for 3 min. After staining, the excess solution was removed, and the grid was allowed to dry for 10 min before storage for future TEM observation at 80 kV.

#### 4.9 | Single-particle interferometric reflectance imaging sensing: ExoView analysis

Single Particle Interferometric Reflectance Imaging Sensing (SP-IRIS) with the ExoView R100 system and the ExoView Human Tetraspanin Kit (NanoView Biosciences, USA) was used. Each testing article was incubated on an ExoView Tetraspanin Chip for 16 h at room temperature, followed by three washes in solution A (ExoView Human Tetraspanin Kit, NanoView Biosciences, USA). Pre-diluted immunocapture antibodies (anti-CD9 CF488, anti-CD81 CF555 and anti-CD63 CF647) were used at a 1:500 dilution in solution A. To achieve the correct antibody concentration, 250  $\mu$ L of the antibody solution were mixed with the remaining 250  $\mu$ L of solution A after chip washing, resulting in a final antibody dilution of 1:1000 for incubation. After a 1-h

incubation at room temperature, the chips were washed, dried and imaged using the ExoView R100 reader and ExoView Scanner 3.0 acquisition software, and the data were subsequently analyzed using the ExoView Analyzer 3.0. (Leung et al., 2024).

#### 4.10 | Bead-based multiplex flow cytometry assay (MACSplex) analysis

A MACSplex human Exosome kit (Miltenyi Biotec, Bergisch-Gladbach, Germany) was used, following the manufacturer's protocol, to assess the expanded surface protein markers of sEV. The sEV were captured using 37 distinct surface marker antibodies (CD1c, CD2, CD3, CD4, CD8, CD9, CD11c, CD14, CD19, CD20, CD24, CD25, CD29, CD31, CD40, CD41b, CD42a, CD44, CD45, CD49e, CD56, CD62p, CD63, CD69, CD81, CD86, CD105, CD133.1, CD142, CD146, CD209, CD326, HLA-ABC, HLA-DR DP DQ, MCSP, ROR1 and SSEA-4) simultaneously and include the two isotype controls (mIgG1 and REA control) corresponding to the antibodies conjugated with fluorescent beads and then analyzed via flow cytometry. The processed samples were run on a Cytex Aurora Flow Cytometer (Cytex Biosciences, USA) and analyzed with SpectroFlo software (Cytex Biosciences, USA) (Leung et al., 2024).

#### 4.11 | Protein concentration analysis

The recovered sEV were lysed by mixing 5  $\mu$ L of each testing article with 5  $\mu$ L of 2 $\times$  RIPA buffer. Protein concentrations of the lysed sEV preparations were quantified using the Pierce™ BCA Protein Assay Kit (Thermo Fisher Scientific, USA), following the manufacturer's protocols.

#### 4.12 | Small EVs RNA isolation and miRNA arrays

Total RNA was extracted from isolated EVs using Norgen's Plasma/Serum RNA Purification Mini Kit (Norgen Biotek Corp.) following the manufacturer's recommendation for RNA extraction from isolated vesicles. RNA concentrations were determined by Quant-It RNA fluorometric assay (Life Technologies). The isolated RNA was reverse transcribed with the TaqMan Advanced miRNA cDNA synthesis kit, following manufacturer instructions, which include an amplification step. The cDNA was then assessed loaded on TaqMan Advanced miRNA Human A and B Cards and the qPCR was performed on a QuantStudio 7 Flex instrument (Life Technologies). For the data analysis, the Ct value of an endogenous control gene (cel-miR-39-3p) was used to normalize the corresponding Ct values for the target genes. Since a Ct value of 30 represents single molecule template detection, Ct values > 30 were considered to be below the detection level of the assay. Therefore, only the miRNAs with a Ct  $\leq$  30 were included in the analyses.

#### 4.13 | Bioinformatics and pathway analysis

Cytoscape was used to construct and visualize mature-dependent miRNA-gene target-disrupted pathway interactions, while R-studio functions were employed to generate heatmaps displaying miRNA overlapping pathways for each group of statistically significant pathways. Normalization of data and generation of correlation plot was done using Thermo Fisher software (Applied biosystems, Thermo Fisher).

To investigate the functional implications of highly expressed miRNAs, those with Ct  $\leq$  30 were initially considered, but only miRNAs with a Ct value cut-off of 25 were analyzed further. The experimentally confirmed gene targets from the miRBase database, supported by literature references, were retrieved using The Ingenuity Knowledge Base as a reference set.

Target gene sets for each group's significant miRNAs were combined and studied for overrepresentation in documented functional gene sets. Ingenuity Pathway Analysis (IPA) identified impacted pathways, regulatory interactions and networks, with KEGG molecular interaction maps retrieved for significant pathways (Krämer et al., 2014). Additional information on significant miRNAs and their target pathways was obtained using In-Silico Construction of an Entity-based Network from Text (IRIDESCENT), a proprietary software scanning MEDLINE (Wren et al., 2004; Wren & Garner, 2004).

#### 4.14 | Statistical analysis

Unless specified otherwise, data are presented as mean  $\pm$  standard deviation (SD). Statistical analysis and graph plotting were performed using GraphPad Prism. Student's *t*-test was utilized to compare the two groups, and significance was defined as *p*-value < 0.05.

## AUTHOR CONTRIBUTIONS

**Dimitrios Pollalis:** Data curation (lead); formal analysis (lead); investigation (lead); methodology (lead); validation (equal); writing—original draft (lead); writing—review and editing (lead). **Gopa Kumar Gopinadhan Nair:** Data curation (lead); formal analysis (equal); methodology (lead); writing—original draft (supporting); writing—review and editing (supporting). **Justin Leung:** Data curation (equal); formal analysis (equal); methodology (equal); validation (equal); writing—review and editing (supporting). **Clarisa Marie Bloemhof:** Data curation (equal); formal analysis (equal); methodology (equal); software (equal); writing—review and editing (supporting). **Jeffrey K. Bailey:** Data curation (equal); formal analysis (equal); investigation (equal); methodology (equal); validation (equal); writing—original draft (equal); writing—review and editing (supporting). **Britney O. Pennington:** Conceptualization (equal); investigation (equal); methodology (equal); resources (equal); writing—original draft (supporting); writing—review and editing (supporting). **Kaitlin R. Kelly:** Data curation (equal); investigation (supporting); methodology (supporting); resources (equal); writing—original draft (supporting); writing—review and editing (supporting). **Amir I. Khan:** Investigation (supporting); methodology (supporting); resources (supporting); writing—original draft (supporting); writing—review and editing (supporting). **Ashley K. Yeh:** Data curation (supporting); formal analysis (supporting); resources (supporting); writing—original draft (supporting); writing—review and editing (supporting). **Kartik S. Sundaram:** Data curation (supporting); formal analysis (supporting); resources (supporting); writing—original draft (supporting); writing—review and editing (supporting). **Dennis O. Clegg:** Conceptualization (supporting); funding acquisition (supporting); project administration (supporting); resources (supporting); supervision (supporting); writing—original draft (supporting); writing—review and editing (supporting). **Chen-Ching Peng:** Conceptualization (supporting); investigation (supporting); resources (supporting); validation (supporting); writing—original draft (supporting); writing—review and editing (supporting). **Liya Xu:** Conceptualization (supporting); methodology (supporting); supervision (supporting); writing—original draft (supporting); writing—review and editing (supporting). **Constantin Georgescu:** Data curation (lead); formal analysis (lead); methodology (lead); writing—original draft (equal); writing—review and editing (supporting). **Jonathan D. Wren:** Data curation (equal); formal analysis (equal); funding acquisition (supporting); resources (supporting); software (supporting); supervision (equal); writing—original draft (supporting); writing—review and editing (supporting). **Sun Young Lee:** Conceptualization (lead); data curation (equal); formal analysis (equal); funding acquisition (lead); investigation (lead); methodology (equal); project administration (equal); resources (equal); supervision (equal); validation (equal); visualization (equal); writing—original draft (lead); writing—review and editing (lead).

## ACKNOWLEDGEMENTS

The authors thank NRI-MCDB Microscopy Facility Spectral Laser Scanning Confocal (award S10OD010610). The authors thank Extracellular Vesicle Core at Children's Hospital Los Angeles and Paolo Neviani, PhD for their technical assistance.

## CONFLICT OF INTEREST STATEMENT

The authors declare no conflicts of interest.

## ORCID

Clarisa Marie Bloemhof  <https://orcid.org/0009-0009-3708-1186>

Liya Xu  <https://orcid.org/0000-0002-5501-2039>

Sun Young Lee  <https://orcid.org/0000-0003-3771-8799>

## REFERENCES

- Abels, E. R., Maas, S. L. N., Nieland, L., Wei, Z., Cheah, P. S., Tai, E., Kolsteeg, C. J., Dusoswa, S. A., Ting, D. T., Hickman, S., & El Khoury, J. (2019). Glioblastoma-associated microglia reprogramming is mediated by functional transfer of extracellular miR-21. *Cell Reports*, 28, 3105–3119. e7. <https://doi.org/10.1016/j.celrep.2019.08.036>
- Ahluwalia, K., Martinez-Camarillo, J. C., Thomas, B. B., Naik, A., Gonzalez-Calle, A., Pollalis, D., Lebkowski, J., Lee, S. Y., Mitra, D., Louie, S. G., & Humayun, M. S. (2023). Polarized RPE secretome preserves photoreceptors in retinal dystrophic RCS rats. *Cells*, 12, 1689. <https://doi.org/10.3390/cells12131689>
- Ahn, J. Y., Datta, S., Bandeira, E., Cano, M., Mallick, E., Rai, U., Powell, B., Tian, J., Witwer, K. W., Handa, J. T., & Paulaitis, M. E. (2021). Release of extracellular vesicle miR-494-3p by ARPE-19 cells with impaired mitochondria. *Biochimica et Biophysica Acta (BBA)-General Subjects*, 1865, 129598. <https://doi.org/10.1016/j.bbagen.2020.129598>
- Al-Ani, A., Sunba, S., Hafeez, B., Toms, D., & Ungrin, M. (2020). In vitro maturation of retinal pigment epithelium is essential for maintaining high expression of key functional genes. *International Journal of Molecular Sciences*, 21(17), 6066. <https://doi.org/10.3390/ijms21176066>
- Ardekani, A. M., & Naeini, M. M. (2010). The role of microRNAs in human diseases. *Avicenna Journal of Medical Biotechnology*, 2, 161–179.
- Barbato, S., Marrocco, E., Intartaglia, D., Pizzo, M., Asteriti, S., Naso, E., Falanga, D., Bhat, R. S., Meola, N., Carissimo, A., Karali, M., Prosser, H. M., Cangiano, L., Surace, E. M., Banfi, S., & Conte, I. (2017). MiR-211 is essential for adult cone photoreceptor maintenance and visual function. *Scientific Reports*, 7(1), 17004. <https://doi-org.libproxy2.usc.edu/10.1038/s41598-017-17331-z>
- Bennis, A., Jacobs, J. G., Catsburg, L. A. E., Ten Brink, J. B., Koster, C., Schlingemann, R. O., van Meurs, J., Gorgels, T. G. M. F., Moerland, P. D., Heine, V. M., & Bergen, A. A. (2017). Stem cell derived retinal pigment epithelium: The role of pigmentation as maturation marker and gene expression profile comparison with human endogenous retinal pigment epithelium. *Stem Cell Reviews and Reports*, 13(5), 659–669. <https://doi-org.libproxy2.usc.edu/10.1007/s12015-017-9754-0>

- Bian, B., Zhao, C., He, X., Gong, Y., Ren, C., Ge, L., Zeng, Y., Li, Q., Chen, M., Weng, C., & He, J. (2020). Exosomes derived from neural progenitor cells preserve photoreceptors during retinal degeneration by inactivating microglia. *Journal of Extracellular Vesicles*, 9, 1748931. <https://doi.org/10.1080/20013078.2020.1748931>
- Bonsergent, E., Grisard, E., Buchrieser, J., Schwartz, O., Théry, C., & Lavieu, G. (2021). Quantitative characterization of extracellular vesicle uptake and content delivery within mammalian cells. *Nature Communications*, 12, 1864. <https://doi.org/10.1038/s41467-021-22126-y>
- Campello, L., Singh, N., Advani, J., Mondal, A. K., Corso-Díaz, X., & Swaroop, A. (2021). Aging of the retina: Molecular and metabolic turbulences and potential interventions. *Annual Review of Vision Science*, 7, 633–664. <https://doi.org/10.1146/annurev-vision-100419-114940>
- Carthew, R. W., & Sontheimer, E. J. (2009). Origins and mechanisms of miRNAs and siRNAs. *Cell*, 136, 642–655. <https://doi.org/10.1016/j.cell.2009.01.035>
- Croze, R. H., Buchholz, D. E., Radeke, M. J., Thi, W. J., Hu, Q., Coffey, P. J., & Clegg, D. O. (2014). ROCK inhibition extends passage of pluripotent stem cell-derived retinal pigmented epithelium. *Stem Cells Translational Medicine*, 3, 1066–1078. <https://doi.org/10.5966/sctm.2014-0079>
- Davis, R. J., Alam, N. M., Zhao, C., Müller, C., Saini, J. S., Blenkinsop, T. A., Mazzoni, F., Campbell, M., Borden, S. M., Charniga, C. J., Lederman, P. L., Aguilar, V., Naimark, M., Fiske, M., Boles, N., Temple, S., Finnemann, S. C., Prusky, G. T., & Stern, J. H. (2017). The developmental stage of adult human stem cell-derived retinal pigment epithelium cells influences transplant efficacy for vision rescue. *Stem Cell Reports*, 9(1), 42–49. <https://doi.org/10.1016/j.stemcr.2017.05.016>
- de Jong, O. G., Murphy, D. E., Mäger, I., Willms, E., Garcia-Guerra, A., Gitz-Francois, J. J., Lefferts, J., Gupta, D., Steenbeek, S. C., van Rheenen, J., & El Andaloussi, S. (2020). A CRISPR-Cas9-based reporter system for single-cell detection of extracellular vesicle-mediated functional transfer of RNA. *Nature Communications*, 11, 1113. <https://doi.org/10.1038/s41467-020-14977-8>
- Dong, L., Zieren, R. C., Horie, K., Kim, C. J., Mallick, E., Jing, Y., Feng, M., Kuczler, M. D., Green, J., Amend, S. R., & Witwer, K. W. (2020). Comprehensive evaluation of methods for small extracellular vesicles separation from human plasma, urine and cell culture medium. *Journal of Extracellular Vesicles*, 10, e12044. <https://doi.org/10.1002/jev2.12044>
- Dunn, K. C., Aotaki-Keen, A. E., Putkey, F. R., & Hjelmeland, L. M. (1996). ARPE-19, a human retinal pigment epithelial cell line with differentiated properties. *Experimental Eye Research*, 62(2), 155–169. <https://doi.org/10.1006/exer.1996.0020>
- Flores-Bellver, M., Mighty, J., Aparicio-Domingo, S., Li, K. V., Shi, C., Zhou, J., Cobb, H., McGrath, P., Michelis, G., Lenhart, P., & Bilousova, G. (2021). Extracellular vesicles released by human retinal pigment epithelium mediate increased polarised secretion of drusen proteins in response to AMD stressors. *Journal of Extracellular Vesicles*, 10, e12165. <https://doi.org/10.1002/jev2.12165>
- Gelibter, S., Marostica, G., Mandelli, A., Siciliani, S., Podini, P., Finardi, A., & Furlan, R. (2022). The impact of storage on extracellular vesicles: A systematic study. *Journal of Extracellular Vesicles*, 11(2), e12162. <https://doi.org/10.1002/jev2.12162>
- Georgi, S. A., & Reh, T. A. (2010). Dicer is required for the transition from early to late progenitor state in the developing mouse retina. *Journal of Neuroscience*, 30, 4048–4061. <https://doi.org/10.1523/JNEUROSCI.4982-09.2010>
- German, O. L., Buzzi, E., Rotstein, N. P., Rodríguez-Boulan, E., & Politi, L. E. (2008). Retinal pigment epithelial cells promote spatial reorganization and differentiation of retina photoreceptors. *Journal of Neuroscience Research*, 86(16), 3503–3514. <https://doi.org/10.1002/jnr.21813>
- Görgens, A., Corso, G., Hagey, D. W., Jawad Wiklander, R., Gustafsson, M. O., Felldin, U., Lee, Y., Bostancioglu, R. B., Sork, H., Liang, X., Zheng, W., Mohammad, D. K., van de Wakker, S. I., Vader, P., Zickler, A. M., Mamand, D. R., Ma, L., Holme, M. N., Stevens, M. M., ... El Andaloussi, S. (2022). Identification of storage conditions stabilizing extracellular vesicles preparations. *Journal of Extracellular Vesicles*, 11(6), e12238. <https://doi.org/10.1002/jev2.12238>
- Guo, C. J., Cao, X. L., Zhang, Y. F., Yue, K. Y., Han, J., Yan, H., Han, H., & Zheng, M. H. (2023). Exosome-mediated inhibition of microRNA-449a promotes the amplification of mouse retinal progenitor cells and enhances their transplantation in retinal degeneration mouse models. *Molecular Therapy-Nucleic Acids*, 31, 763–778. <https://doi.org/10.1016/j.omtn.2023.02.015>
- Handa, J. T., Bowes Rickman, C., Dick, A. D., Gorin, M. B., Miller, J. W., Toth, C. A., Ueffing, M., Zarbin, M., & Farrer, L. A. (2019). A systems biology approach towards understanding and treating non-neovascular age-related macular degeneration. *Nature Communications*, 10, 3347. <https://doi.org/10.1038/s41467-019-11262-1>
- Intartaglia, D., Giamundo, G., & Conte, I. (2021). The impact of miRNAs in health and disease of retinal pigment epithelium. *Frontiers in Cell and Developmental Biology*, 8, 589985. <https://doi.org/10.3389/fcell.2020.589985>
- Joshi, B. S., de Beer, M. A., Giepmans, B. N. G., & Zuhorn, I. S. (2020). Endocytosis of extracellular vesicles and release of their cargo from endosomes. *ACS Nano*, 14, 4444–4455. <https://doi.org/10.1021/acsnano.9b10033>
- Kashani, A. H., Lebkowski, J. S., Rahhal, F. M., Avery, R. L., Salehi-Had, H., Chen, S., Chan, C., Palejwala, N., Ingram, A., Dang, W., & Lin, C. M. (2021). One-year follow-up in a phase 1/2a clinical trial of an allogeneic RPE cell bioengineered implant for advanced dry age-related macular degeneration. *Translational Visual Science & Technology*, 10, 13. <https://doi.org/10.1167/tvst.10.10.13>
- Kashani, A. H., Lebkowski, J. S., Rahhal, F. M., Avery, R. L., Salehi-Had, H., Dang, W., Lin, C. M., Mitra, D., Zhu, D., Thomas, B. B., & Hikita, S. T. (2018). A bioengineered retinal pigment epithelial monolayer for advanced, dry age-related macular degeneration. *Science Translational Medicine*, 10, ea04097. <https://doi.org/10.1126/scitranslmed.a04097>
- Ke, Y., Fan, X., Hao, R., Dong, L., Xue, M., Tan, L., Yang, C., Li, X., & Ren, X. (2021). Human embryonic stem cell-derived extracellular vesicles alleviate retinal degeneration by upregulating Oct4 to promote retinal Müller cell retrodifferentiation via HSP90. *Stem Cell Research & Therapy*, 12, 21. <https://doi.org/10.1186/s13287-020-02034-6>
- Kim, K. M., Abdelmohsen, K., Mustapic, M., Kapogiannis, D., & Gorospe, M. (2017). RNA in extracellular vesicles. *Wiley Interdisciplinary Reviews: RNA*, 8(4). <https://doi.org/10.1002/wrna.1413>
- Kim, V. N. (2005). MicroRNA biogenesis: Coordinated cropping and dicing. *Nature Reviews Molecular Cell Biology*, 6, 376–385. <https://doi.org/10.1038/nrml644>
- Krämer, A., Green, J., Pollard, J. Jr, & Tugendreich, S. (2014). Causal analysis approaches in Ingenuity Pathway Analysis. *Bioinformatics (Oxford, England)*, 30(4), 523–530. <https://doi.org/10.1093/bioinformatics/btt703>
- Lagos-Quintana, M., Rauhut, R., Yalcin, A., Meyer, J., Lendeckel, W., & Tuschl, T. (2002). Identification of tissue-specific microRNAs from mouse. *Current Biology*, 12, 735–739. [https://doi.org/10.1016/s0960-9822\(02\)00809-6](https://doi.org/10.1016/s0960-9822(02)00809-6)
- La Torre, A., Georgi, S., & Reh, T. A. (2013). Conserved microRNA pathway regulates developmental timing of retinal neurogenesis. *Proceedings of the National Academy of Sciences*, 110, E2362–E2370. <https://doi.org/10.1073/pnas.1301837110>
- Leach, L. L., Croze, R. H., Hu, Q., Nadar, V. P., Clevenger, T. N., Pennington, B. O., Gamm, D. M., & Clegg, D. O. (2016). Induced pluripotent stem cell-derived retinal pigmented epithelium: A comparative study between cell lines and differentiation methods. *Journal of Ocular Pharmacology and Therapeutics*, 32, 317–330. <https://doi.org/10.1089/jop.2016.0022>
- Leung, J., Pollalis, D., Nair, G. K. G., Bailey, J. K., Pennington, B. O., Khan, A. I., Kelly, K. R., Yeh, A. K., Sundaram, K. S., Clegg, D. O., Peng, C. C., Xu, L., & Lee, S. Y. (2024). Isolation and characterization of extracellular vesicles through orthogonal approaches for the development of intraocular EV therapy. *Investigative Ophthalmology & Visual Science*, 65(3), 6. <https://doi.org/10.1167/iovs.65.3.6>

- Ludwig, A. K., & Giebel, B. (2012). Exosomes: Small vesicles participating in intercellular communication. *International Journal of Biochemistry & Cell Biology*, 44, 11–15. <https://doi.org/10.1016/j.biocel.2011.10.005>
- Mandai, M., Kurimoto, Y., & Takahashi, M. (2017). Autologous induced stem-cell-derived retinal cells for macular degeneration. *New England Journal of Medicine*, 377, 792–793. <https://doi.org/10.1056/NEJMc1706274>
- Mathew, B., Ravindran, S., Liu, X., Torres, L., Chennakesavalu, M., Huang, C. C., Feng, L., Zelka, R., Lopez, J., Sharma, M., & Roth, S. (2019). Mesenchymal stem cell-derived extracellular vesicles and retinal ischemia-reperfusion. *Biomaterials*, 197, 146–160. <https://doi.org/10.1016/j.biomaterials.2019.01.016>
- Mehat, M. S., Sundaram, V., Ripamonti, C., Robson, A. G., Smith, A. J., Borooah, S., Robinson, M., Rosenthal, A. N., Innes, W., Weleber, R. G., & Lee, R. W. (2018). Transplantation of human embryonic stem cell-derived retinal pigment epithelial cells in macular degeneration. *Ophthalmology*, 125, 1765–1775. <https://doi.org/10.1016/j.ophtha.2018.04.037>
- Meyer, J. G., Garcia, T. Y., Schilling, B., Gibson, B. W., & Lamba, D. A. (2019). Proteome and secretome dynamics of human retinal pigment epithelium in response to reactive oxygen species. *Scientific reports*, 9(1), 15440. <https://doi.org/10.1038/s41598-019-51777-7>
- Morris, D. R., Bounds, S. E., Liu, H., Ding, W. Q., Chen, Y., Liu, Y., & Cai, J. (2020). Exosomal MiRNA transfer between retinal microglia and RPE. *International Journal of Molecular Sciences*, 21, 3541. <https://doi.org/10.3390/ijms21103541>
- Nair, G. K. G., Pollalis, D., Wren, J. D., Georgescu, C., Sjoelund, V., & Lee, S. Y. (2022). Proteomic insight into the role of exosomes in proliferative vitreoretinopathy development. *Journal of Clinical Medicine*, 11, 2716. <https://doi.org/10.3390/jcm11102716>
- Petrus-Reurer, S., Lederer, A. R., Baqué-Vidal, L., Douagi, I., Pannagel, B., Khven, I., Aronsson, M., Bartuma, H., Wagner, M., Wrona, A., & Efstathopoulos, P. (2022). Molecular profiling of stem cell-derived retinal pigment epithelial cell differentiation established for clinical translation. *Stem Cell Reports*, 17, 1458–1475. <https://doi.org/10.1016/j.stemcr.2022.05.005>
- Pollalis, D., Calle, A. G., Martinez-Camarillo, J. C., Ahluwalia, K., Hinman, C., Mitra, D., Lebkowski, J., Lee, S. Y., Thomas, B. B., Ahmed, F., Chan, V., Junge, J. A., Fraser, S., Louie, S., & Humayun, M. (2024). Scaling up polarized RPE cell supernatant production on parylene membrane. *Experimental Eye Research*, 240, 109789. <https://doi-org.libproxy2.usc.edu/10.1016/j.exer.2024.109789>
- Ratajczak, J., Wysoczynski, M., Hayek, F., Janowska-Wieczorek, A., & Ratajczak, M. Z. (2006). Membrane-derived microvesicles: important and underappreciated mediators of cell-to-cell communication. *Leukemia*, 20, 1487–1495. <https://doi.org/10.1038/sj.leu.2404296>
- Schwartz, S. D., Regillo, C. D., Lam, B. L., Elliott, D., Rosenfeld, P. J., Gregori, N. Z., Hubschman, J. P., Davis, J. L., Heilwell, G., Sporn, M., & Maguire, J. (2015). Human embryonic stem cell-derived retinal pigment epithelium in patients with age-related macular degeneration and Stargardt's macular dystrophy: Follow-up of two open-label phase 1/2 studies. *Lancet*, 385, 509–516. [https://doi.org/10.1016/S0140-6736\(14\)61376-3](https://doi.org/10.1016/S0140-6736(14)61376-3)
- Strauss, O. (2005). The retinal pigment epithelium in visual function. *Physiological Reviews*, 85, 845–881. <https://doi.org/10.1152/physrev.00021.2004>
- Vaka, R., Parent, S., Risha, Y., Khan, S., Courtman, D., Stewart, D. J., & Davis, D. R. (2023). Extracellular vesicle microRNA and protein cargo profiling in three clinical-grade stem cell products reveals key functional pathways. *Molecular Therapy-Nucleic Acids*, 32, 80–93. <https://doi.org/10.1016/j.omtn.2023.03.001>
- van der Pol, E., Böing, A. N., Harrison, P., Sturk, A., & Nieuwland, R. (2012). Classification, functions, and clinical relevance of extracellular vesicles. *Pharmacological Reviews*, 64, 676–705. <https://doi.org/10.1124/pr.112.005983>
- Wang, F. E., Zhang, C., Maminishkis, A., Dong, L., Zhi, C., Li, R., Zhao, J., Majerciak, V., Gaur, A. B., Chen, S., & Miller, S. S. (2010). MicroRNA-204/211 alters epithelial physiology. *The FASEB Journal*, 24(5), 1552–1571. <https://doi-org.libproxy2.usc.edu/10.1096/fj.08-125856>
- Wang, H. C., Greene, W. A., Kaini, R. R., Shen-Gunther, J., Chen, H. I., Cai, H., & Wang, Y. (2014). Profiling the microRNA expression in human iPSC and iPSC-derived retinal pigment epithelium. *Cancer Informatics*, 13(Suppl 5), 25–35. <https://doi-org.libproxy2.usc.edu/10.4137/CIN.S14074>
- Webber, J., & Clayton, A. (2013). How pure are your vesicles. *Journal of Extracellular Vesicles*, 10:2. <https://doi-org.libproxy2.usc.edu/10.3402/jev.v2i0.19861>
- Woo, H. K., Sunkara, V., Park, J., Kim, T. H., Han, J. R., Kim, C. J., Choi, H. I., Kim, Y. K., & Cho, Y. K. (2017). Exodisc for rapid, size-selective, and efficient isolation and analysis of nanoscale extracellular vesicles from biological samples. *ACS Nano*, 11, 1360–1370. <https://doi.org/10.1021/acsnano.6b06131>
- Wooff, Y., Cioanca, A. V., Chu-Tan, J. A., Aggio-Bruce, R., Schumann, U., & Natoli, R. (2020). Small-medium extracellular vesicles and their miRNA cargo in retinal health and degeneration: Mediators of homeostasis, and vehicles for targeted gene therapy. *Frontiers in Cellular Neuroscience*, 14, 160. <https://doi.org/10.3389/fncel.2020.00160>
- Wren, J. D., Bekeredjian, R., Stewart, J. A., Shohet, R. V., & Garner, H. R. (2004). Knowledge discovery by automated identification and ranking of implicit relationships. *Bioinformatics*, 20(3), 389–398. <https://doi.org/10.1093/bioinformatics/btg421>
- Wren, J. D., & Garner, H. R. (2004). Shared relationship analysis: Ranking set cohesion and commonalities within a literature-derived relationship network. *Bioinformatics*, 20(2), 191–198. <https://doi.org/10.1093/bioinformatics/btg390>
- Wright, C. B., Uehara, H., Kim, Y., Yasuma, T., Yasuma, R., Hirahara, S., Makin, R. D., Apicella, I., Pereira, F., Nagasaka, Y., & Narendran, S. (2020). Chronic Dicer1 deficiency promotes atrophic and neovascular outer retinal pathologies in mice. *Proceedings of the National Academy of Sciences*, 117, 2579–2587. <https://doi.org/10.1073/pnas.1909761117>
- Yuan, Z., Ding, S., Yan, M., Zhu, X., Liu, L., Tan, S., Jin, Y., Sun, Y., Li, Y., & Huang, T. (2015). Variability of miRNA expression during the differentiation of human embryonic stem cells into retinal pigment epithelial cells. *Gene*, 569, 239–249. <https://doi.org/10.1016/j.gene.2015.05.060>
- Zhang, C., Miyagishima, K. J., Dong, L., Rising, A., Nimmagadda, M., Liang, G., Sharma, R., Dejene, R., Wang, Y., Abu-Asab, M., Qian, H., Li, Y., Kopera, M., Maminishkis, A., Martinez, J., & Miller, S. (2019). Regulation of phagolysosomal activity by miR-204 critically influences structure and function of retinal pigment epithelium/retina. *Human Molecular Genetics*, 28(20), 3355–3368. <https://doi-org.libproxy2.usc.edu/10.1093/hmg/ddz171>

## SUPPORTING INFORMATION

Additional supporting information can be found online in the Supporting Information section at the end of this article.

**How to cite this article:** Pollalis, D., Nair, G. K. G., Leung, J., Bloemhof, C. M., Bailey, J. K., Pennington, B. O., Kelly, K. R., Khan, A. I., Yeh, A. K., Sundaram, K. S., Clegg, D. O., Peng, C.-C., Xu, L., Georgescu, C., Wren, J. D., & Lee, S. Y. (2024). Dynamics of microRNA secreted via extracellular vesicles during the maturation of embryonic stem cell-derived retinal pigment epithelium. *Journal of Extracellular Biology*, 3, e70001. <https://doi.org/10.1002/jex2.70001>